# Passive and active launch vibration studies in the LVIS program

Donald L Edberg[a] , Bruce Bartos[a], James Goodding[b], Paul Wilke[b], Torey Davis[c]

[a]Boeing, 5301 Bolsa Ave, MS H013-C316, Huntington Beach, CA 92647
[b]CSA Engineering Inc., Palo Alto, CA
[c]Honeywell Satellite Systems Operation, Phoenix, AZ

## ABSTRACT

A U.S. Air Force-sponsored team consisting of Boeing (formerly McDonnell Douglas), Honeywell Satellite Systems, and CSA Engineering has developed technology to reduce the vibration felt by an isolated payload during launch. Spacecraft designers indicate that a launch vibration isolation system (LVIS) could provide significant cost benefits in payload design, testing, launch, and lifetime. This paper contains developments occurring since those reported previously[1].

Simulations, which included models of a 6,500 pound spacecraft, an isolating payload attach fitting (PAF) to replace an existing PAF, and the Boeing Delta II launch vehicle, were used to generate PAF performance requirements for the desired levels of attenuation. Hardware was designed to meet the requirements. The isolating PAF concept replaces portions of a conventional metallic fitting with hydraulic-pneumatic struts featuring a unique hydraulic cross-link feature that stiffens under rotation to meet rocking restrictions. The pneumatics provide low-stiffness longitudinal support.

Two demonstration isolating PAF struts were designed, fabricated, and tested to determine their stiffness and damping characteristics and to verify the performance of the hydraulic crosslink concept. Measurements matched analytical predictions closely. An active closed-loop control system was simulated to assess its potential isolation performance. A factor of 100 performance increase over the passive case was achieved with minor weight addition and minimal power consumption.

**Keywords:** vibration isolation, attenuation, launch vehicle, payload attach fitting.

## 1. LVIS CONCEPT DESCRIPTION

Figure 1 depicts a spacecraft on its payload adaptor fitting (PAF). The PAF is rigidly connected to both the spacecraft and the launch vehicle and provides minimal attenuation of vibrations being applied at its base. In most cases, all loads are transmitted directly to the payload; occasionally special modifications have been made to provide attenuation for specific resonances. LVIS' goal is to provide 80% attenuation of the RMS axial and lateral vibrations in the 20-40 Hz regime.

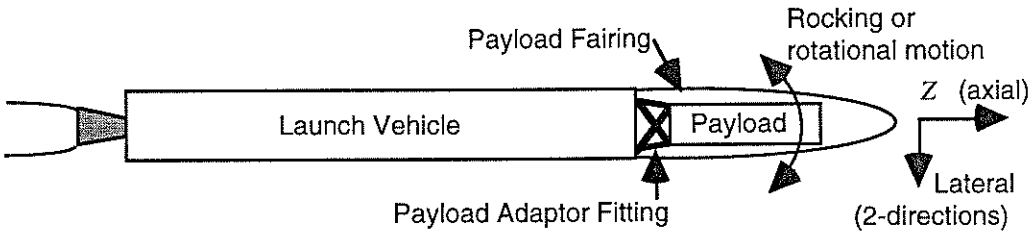


Figure 1. Arrangement of launch vehicle, PAF, and spacecraft, with coordinate systems definition.

Further author information —
D.L.E. (correspondence): Email: don.edberg@boeing.com; telephone 1-714-896-5210; FAX 1-714-896-2305.
B.B.: email bruce.bartos@boeing.com. J.G.: email gooddinj@plk.af.mil. PW: email: wilke@csaengr.com. TD.: email: tdavis@space.honeywell.com.

# Report Documentation Page

*Form Approved*
*OMB No. 0704-0188*



| 1. REPORT DATE | 2. REPORT TYPE | 3. DATES COVERED |
|---|---|---|
| **1998** | | **00-00-1998 to 00-00-1998** |

| 4. TITLE AND SUBTITLE | 5a. CONTRACT NUMBER |
|---|---|
| **Passive and active launch vibration studies in the LVIS program** | 5b. GRANT NUMBER |
| | 5c. PROGRAM ELEMENT NUMBER |
| 6. AUTHOR(S) | 5d. PROJECT NUMBER |
| | 5e. TASK NUMBER |
| | 5f. WORK UNIT NUMBER |
| 7. PERFORMING ORGANIZATION NAME(S) AND ADDRESS(ES)<br>**CSA Engineering,2565 Leghorn Street,Mountain View,CA,94043** | 8. PERFORMING ORGANIZATION REPORT NUMBER |
| 9. SPONSORING/MONITORING AGENCY NAME(S) AND ADDRESS(ES) | 10. SPONSOR/MONITOR'S ACRONYM(S) |
| | 11. SPONSOR/MONITOR'S REPORT NUMBER(S) |

12. DISTRIBUTION/AVAILABILITY STATEMENT
**Approved for public release; distribution unlimited**

13. SUPPLEMENTARY NOTES

14. ABSTRACT
**see report**

15. SUBJECT TERMS

| 16. SECURITY CLASSIFICATION OF: | | | 17. LIMITATION OF ABSTRACT | 18. NUMBER OF PAGES | 19a. NAME OF RESPONSIBLE PERSON |
|---|---|---|---|---|---|
| a. REPORT | b. ABSTRACT | c. THIS PAGE | | | |
| **unclassified** | **unclassified** | **unclassified** | | **12** | |

**Standard Form 298 (Rev. 8-98)**
Prescribed by ANSI Std Z39-18

Although the axial loading caused by the launch vehicle's steady axial acceleration provides the largest magnitude of loading during flight, there are also lateral loads which occur primarily due to maneuvers initiated by the vehicle's guidance system and encounters with wind shear situations. The lateral loading excites the launch vehicle's body bending modes which drive the payload's lateral displacements ("rocking" motion), possibly causing undesirable contact with the payload fairing.

Since the payload's mass center is generally far forward of the PAF, the clearance requirements at the inside of the payload fairing force the PAF to have very high rocking stiffness. The conflicting requirements of low axial stiffness to attenuate axial vibrations along with high rocking stiffness to achieve payload fairing clearance requirements make the LVIS design particularly challenging.

## 2. LVIS ANALYTICAL MODELLING

The LVIS system simulations utilized finite-element models for a liftoff-configuration Delta II launch vehicle, several payload attach fittings, and a spacecraft. A PAF model is shown in Figure 2. The upper and lower rings represent the actual structure of a model 6915[2] Delta PAF. In order to allow us to easily modify the dynamics of the isolating PAF, the isolating struts connecting the two rings are modeled as bar elements. The isolating LVIS strut elements could be individually modified to change their stiffness and damping (and to implement active control if desired) to represent various isolating PAF configurations.

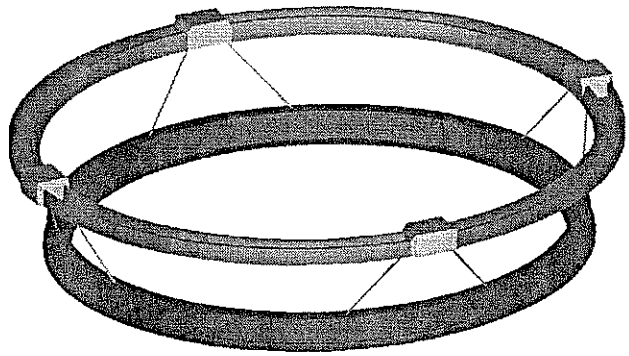

Figure 2. Finite element model of payload attach fitting.

A baseline configuration mimicking the standard Delta PAF was utilized for comparison purposes. A second configuration modelled the LVIS dynamics, including the effects of incorporating hydraulically cross-linked struts to provide enhanced rocking stiffness. The detailed design could not proceed with first carrying out simulations whose results would be used to assess the LVIS' isolation performance.

A transfer function approach was used to assess the performance and isolation benefits of candidate LVIS systems[1]. A number of simulations computing the response at the satellite top due to axial forcing applied at the main engine location were run in order to generate a family of RMS ratio curves as a function of the axial isolation frequencies (whole spacecraft fixed-base axial frequencies). A 5 Hz axial frequency was found to provide good isolation. The simulations showed a definite response reduction over the broad band due to the LVIS' presence, if tuned to certain frequencies.

The result of selecting a 5 Hz axial isolation frequency (fixed-base frequency) indicates benefits in the RMS value of transient acceleration over a wide frequency band due to liftoff loads. For the 20 – 40 Hz band, an 80% RMS acceleration reduction is achieved. Acceleration from 0 – 40 Hz is reduced by 60%. Note that these results include the axial LVIS parametsrs only , and even higher benefits will be achieved once lateral isolation is incorporated.

## 3. LVIS HARDWARE IMPLEMENTATION

The LVIS isolator concept uses special elements to connect the top and bottom rings of the PAF shown in Figure 2. Based on a conservative loads assessment, the LVIS strut elements have been sized at 87.6 MN/m (500 klbf/in) and provide up to 3.8 cm (1.5 in) allowable axial displacement. The analysis indicated that the eight struts need to be

arranged in such a manner as to provide a 5 Hz suspension frequency in the axial degree of freedom with the isolator base fixed.

Our mechanical design effort yielded a LVIS strut concept utilizing a pneumatic means of "offloading" the static weight of the payload, so that future implementations of active control methods will not have to provide the static offloading forces (Figure 3a). One benefit of using a pneumatic support is that the element forces needed to support the payload may be supplied by the internal gas' cylinder pressure, and may be easily adapted to payloads of varying mass (or tailored to the varying acceleration during boost) by simply adjusting its internal pressure.

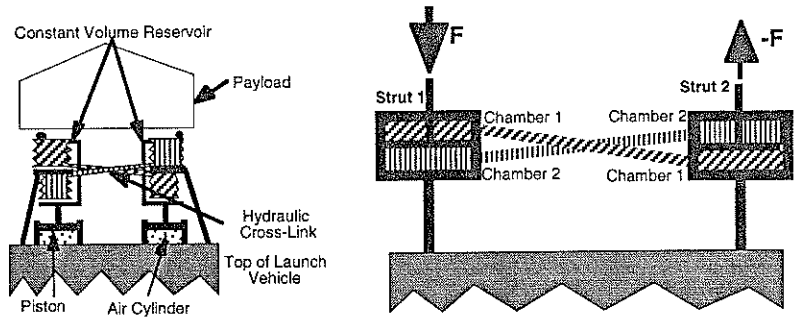


Figure 3a & b. Pneumatic offloading isolation concept for LVIS strut member; schematic of hydraulics of cross-linked struts.

The rotational or rocking degrees of freedom are stiffened significantly by a unique hydraulic cross-linking system which provides two important features: first, its constant-volume reservoir serves as a hydraulic feedback system providing exceptional rocking stiffness. Secondly, it provides both low stiffness and substantial damping for axial motion of the payload. These features are crucial to the proper performance of the LVIS system.

The cross-linking system may be understood by examining Figure 3b. Under a pure static rotation, idealized as a pair of forces acting about equal moment arms, Strut 1 experiences a purely compressive load and Strut 2 experiences a purely tensile load. Under the conditions depicted in Figure 3b, hydraulic fluid in Chamber 1 of Strut 1 is forced to flow to Chamber 2 of Strut 2. However, because a tensile load is experienced by Strut 2, the motion of the hydraulic piston in Strut 2 opposes the net flow of the fluid from Strut 1. Presumably, since the pressures in the two chambers equilibrate, there can be no net fluid flow between the hydraulic chambers. This fact, together with the incompressibility of the hydraulic fluid, implies that there can be no net relative motion between the strut pistons, causing extreme resistance to rotation..

Figure 4 shows a cross-section of the LVIS strut design and a photograph of the actual hardware. Weight estimates for one strut predict around 7 to 9 kg (15 to 20 lbf) for each unit. We did not attempt to attain this weight, since our primary goal was to design and build a strut to demonstrate the cross-linking technology. Refinements were planned for continuing work.

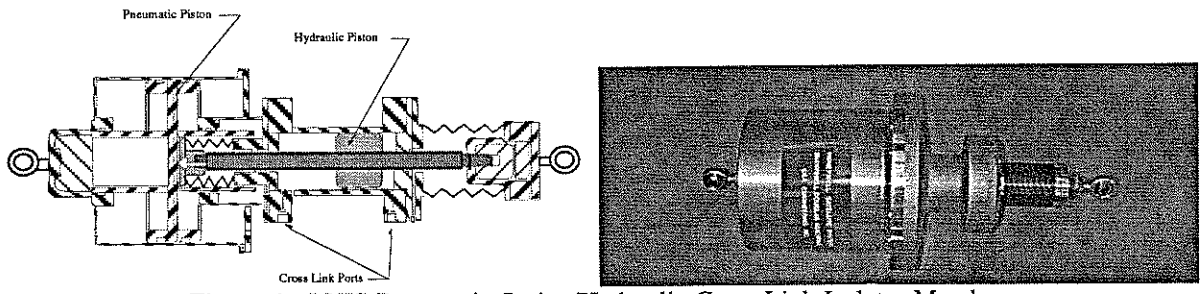


Figure 4. LVIS Pneumatic Spring/Hydraulic Cross-Link Isolator Member.

## 4. TESTING

The LVIS program carried out a series of tests on the two LVIS strut elements in order to determine isolator strut performance and compare with predictions. To understand the pneumatic system's performance, we tested a single LVIS strut; to measure the "rocking" stiffness of the LVIS system, we used a pair of LVIS struts with their hydraulic systems crosslinked.

The testing objectives were to measure the strut's pneumatic stiffness under both quasi-static conditions and several frequencies as well as any static relaxation; to measure the hydraulically cross-linked struts' rocking stiffness; to measure the surge and rocking direction direct complex stiffness; and to quantify the damping caused by fluid flow through the hydraulic circuit in the non-crosslinked configuration. All of these test objectives were accomplished and the struts behaved as designed. The functionality of the LVIS isolating strut concept combining a high capacity air-spring isolator with a rotationally-stiffening hydraulic damping system was demonstrated.

As shown in Figure 5, the strut or struts were situated between the ram of a servohydraulic actuator and the strain gauge load cell. The load cell measured the force transmitted through the strut, and a set of non-contacting eddy current sensors measured displacement. Excitation control was provided by an electronic closed-loop control commanding displacement. The actuator was commanded in its displacement mode to apply forcing to the end of the strut or struts, and the resulting displacement was measured as a function of time to determine the struts' actual physical parameters (the displacement mode uses an integral LVDT displacement sensor in the actuator as the feedback element). To ensure good seal surfaces, a "seal burn-in" was performed by oscillating each strut over nearly its entire stroke at a low frequency before the testing commenced.

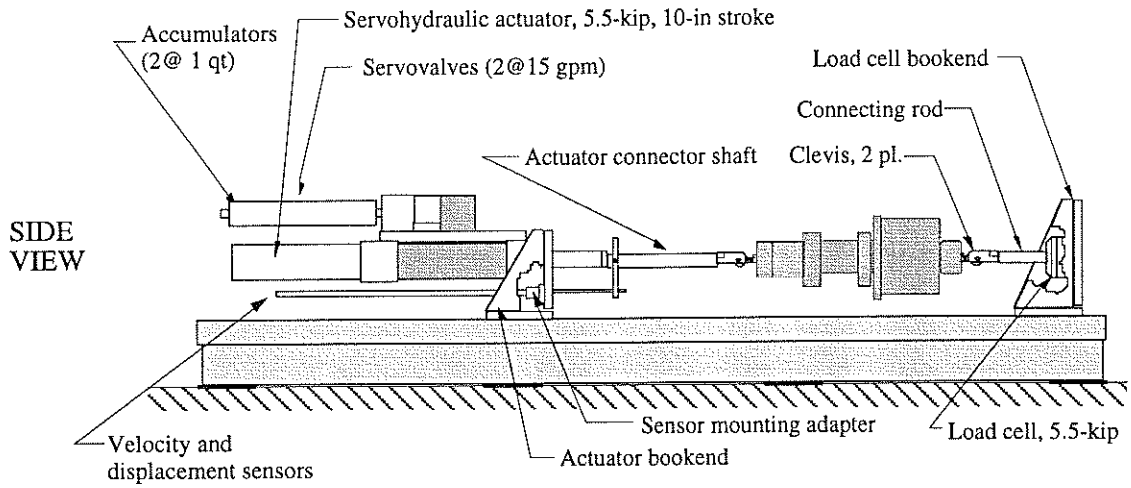


Figure 5. Lab setup for single-strut stiffness testing.

Because the force transmitted through the strut may be a nonlinear function of both the stroke and stroke velocity across the strut, the amplitude and frequency of the input sinusoid were varied from test to test. By comparing the input displacement and output force waveforms, the strut parameters may then be characterized. Figure 6 shows the component testing under way within a plywood safety enclosure known as "Graceland".

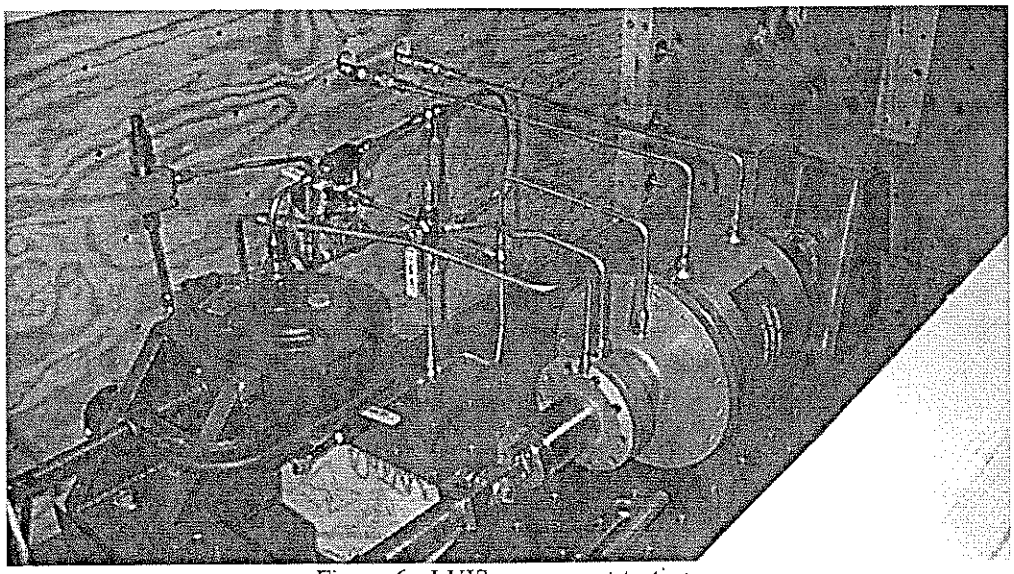

Figure 6. LVIS component testing.

**Relaxation measurements.** Static relaxation measurements determined the leak rate of the pneumatic and hydraulic systems. A single strut was either compressed or elongated to produce a desired initial load through the strut. This deflection was maintained, and the resulting load measured over a long time period to observe the load relaxation over time.

Figure 7 shows load relaxation plots measured on the two LVIS struts with the air springs carrying the load. Both struts were subjected to compressive loads, starting from roughly 2250 $lb_f$ in these two experiments. The pneumatic spring design performed as expected with starting spring rates very near 4000 $lb_f$/in and increasing with stroke. The load through the strut drops off as time progresses, a sign of leakage through the pneumatic cylinder's seals. Within about 30 seconds, the leakage has caused the pressures on either side of the piston to become equal. This leakage is undesirable because it would require a larger $N_2$ tank and more complex plumbing at the system level.

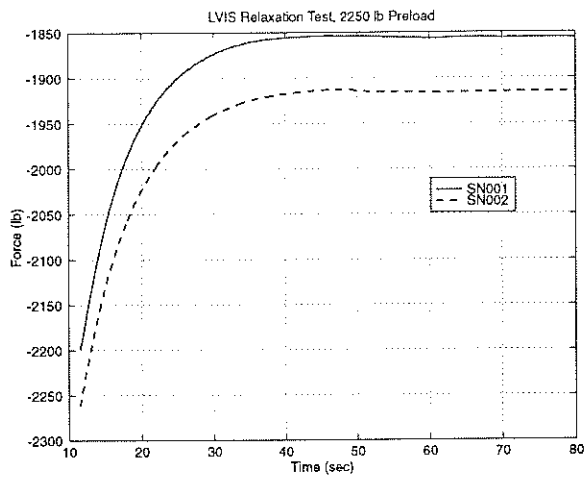


Figure 7. Pneumatic spring load relaxation plots

The seal leakage was was caused by the surface condition at the cylinder/seal interface, which did not meet the manufacturer's recommended surface finish. Since the LVIS struts were concept validation units and not flight units, we opted to assemble under this condition, with the risk that there might be more leakage due to the rougher surface.

Note that each strut is asymptotic to a force due to the different projected area on the two sides of the air piston: the air piston is of a single-rod design. The pneumatic springs utilize air's compressibility to provide static stiffness and

payload support. The addition of pressure into either or both of the two chambers makes it possible to change the strut stiffness without changing the supported load, which differentiates the LVIS strut from the more common single-chamber air spring isolators.

**Quasi-static measurements.** Quasi-static measurements were made by commanding a very low frequency sine (about 0.1 Hz) to the actuator. This limits the contributions due to line losses caused by flow through the hydraulic circuit. Other measurements were made at one, five and ten Hz to determine the time domain strut characteristics at increased frequencies.

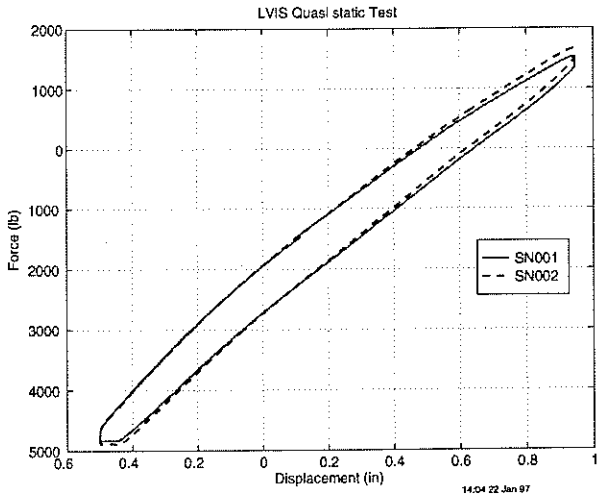


Figure 8. Quasi-static orbit plots

The time domain functions appearing are so-called "orbit plots." Ordinate values are load signals, calibrated in $lb_f$. The abscissa is the strut deformation. When parameterized with time, this can be used to determine the amount of damping (related to the enclosed area in the hysteresis loop) and the stiffness (the slope of the major axis of the hysteresis loop).

Figure 8 shows orbit plots from quasi-static measurements made on both struts with the air springs plumbed. The two curves' similarity indicates nearly identical stiffnesses. The vertical jumps at the ends of the loops are evidence of sliding friction. The abrupt displacement changes with little change in force at the highly-loaded condition (lower left corner of the orbit) indicate the presence of a deadband-type phenomenon believed to be caused by pneumatic piston seal "roll-over".

Sliding friction between 100 and 200 $lb_f$ was measured in the struts during the component testing. This friction was anticipated and is not expected to pose any significant performance problems for the 8,700 $lb_f$ capacity component. Other than the changes in surface finish described earlier, no design changes are planned to reduce the sliding seal stiction of the flight LVIS struts.

**Direct Complex Stiffness.** Direct complex stiffness (DCS) testing was performed to characterize the frequency-dependence of the stiffness and damping and to determine the magnitude of any friction due to sliding seals. It provides the tangent stiffness and loss factor as a function of static preload. Our testing biased the load on the struts to demonstrate their structural integrity under the equivalent of a 6 g static preload.

DCS measurements consist of frequency response functions (FRFs) relating the resulting change in strut length as a function of the imposed load across the strut, and are based on the assumption that the LVIS strut behaves linearly. A number of factors in the strut design have nonlinear behavior, but the DCS functions are a good indication of the strut performance based on small deformations.

FRFs were downloaded to MATLAB for post-processing, where it was assumed that the strut behaved as a parallel combination of a linear spring and a dashpot. Force through the spring was assumed to be proportional to displacement. The stiffness was assumed to be the low frequency asymptote of the magnitude of the X/F plot. Force through the

dashpot was assumed to be proportional to velocity. The ratio of dashpot force to spring force can then be inferred from the phase of the complex compliance and the spring stiffness. The relationship is

$$C(f) = -\frac{k}{2\pi f}\tan\left[q(f)\right]$$

where $C(f)$ = damper force/velocity ratio at frequency $f$, (units $lb_f$-sec/in), $f$ = frequency (Hz); $k$ = spring stiffness ($lb_f$/in); and $q(f)$ = phase of displacement relative to force at frequency $f$.

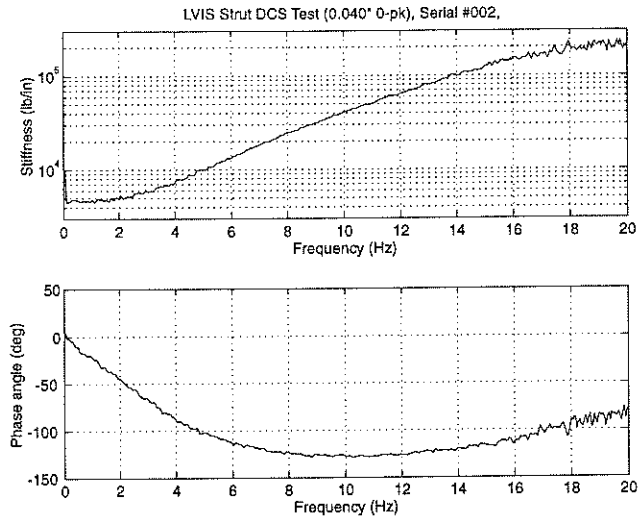


Figure 9. Strut #2 direct complex stiffness

Figure 9 shows the measured direct complex stiffness for the LVIS strut serial number 002. The stiffness varies from roughly 3,000 $lb_f$/in at low frequencies to 200,000 $lb_f$/in near 20 Hz. Contributions to this stiffness from the hydraulic circuit must account for this stiffness variation, as it is unexpected for a pure air spring. The change in phase angle at relatively low frequencies is an indication of the role that the loss due to fluid flow is playing on the strut dynamic characteristic.

**Single-Strut Hydraulic Testing.** As shown in Figure 10a&b, test results for this strut showed a 138,000 $lb_f$/in stiffness in compression and an 86,000 $lb_f$/in stiffness in tension. The compression data show excellent correlation with the predicted analysis value (148,000 $lb_f$/in), but the tension side data apparently show the effects of a small leak in either the tension-side piston seal or shaft seal.

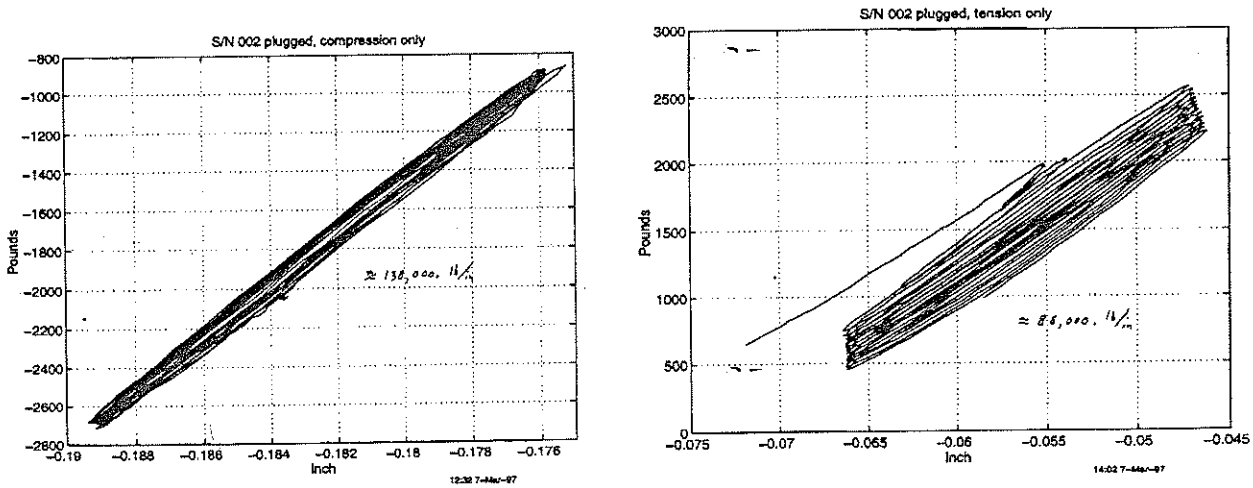


Figure 10. LVIS single strut stiffness test data in compression (left) shows excellent linearity and as-predicted stiffness; data in tension (right) show high stiffness but also indications of a sliding seal leak.

**System-Level Testing.** Tests on an individual strut do not reflect the anti-rocking behavior of the crosslinked struts, so we chose to carry out testing on the two struts with hydraulic crosslinking. Tests were performed with two struts configured with a pivoted load beam connected to the strut moving ends, as shown in Figure 11. This arrangement generates loads similar to that associated with the in-service arrangement, where struts would be crosslinked to to those on the opposite side of a PAF. In this setup, a load cell was affixed to the rod end bearing on the non-moving end of a strut, and displacement probes were used to measure the strut deformation. The tests were static in nature so that the load measured across one of the struts is equivalent the load applied to both struts. The orbit plots of the transduced measurements of load and deflection presented below were generated to compute the cross-link stiffness.

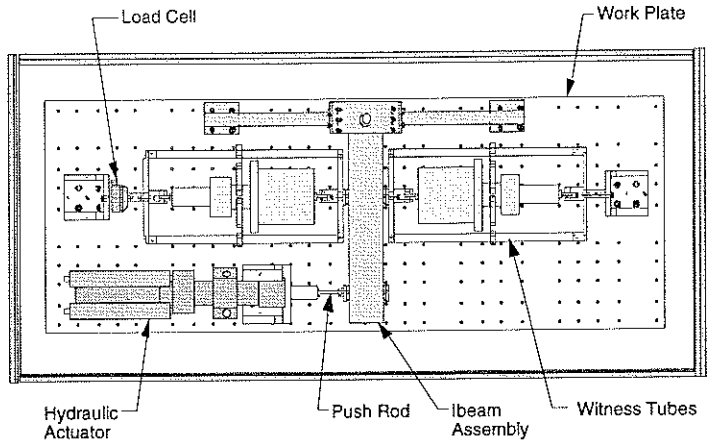


Figure 11. Collinear opposed strut (crosslink) test setup.

Tthe high rotational stiffness created by the struts arises as a result of the hydraulic cross-linking between the struts. Under a pure rotation, the hydraulic load generated by a compressive load in one of the struts is equal in magnitude to the tensile load experienced by its mate. While the near-incompressibility of the fluid linking the adjacent struts implies that the system is theoretically infinitely stiff in rotation, in reality compliances arise through the elasticity of the hydraulic lines, the compressibility of the hydraulic fluid itself, as well as any residual gas contained within the hydraulic lines. The objective of these tests was to verify that these stray compliances were small and that the net rotational stiffness of pair of cross-linked struts was very high.

The actual system-level test configuration is shown in the photograph in Figure 12. This photo does not show the later position measurement scheme where the displacement sensors were mounted on magnetic bases and their targets were mounted directly to either end of the pair of struts. With the modified displacement sensing, the strut deformation is simply the difference of the two displacement signals.

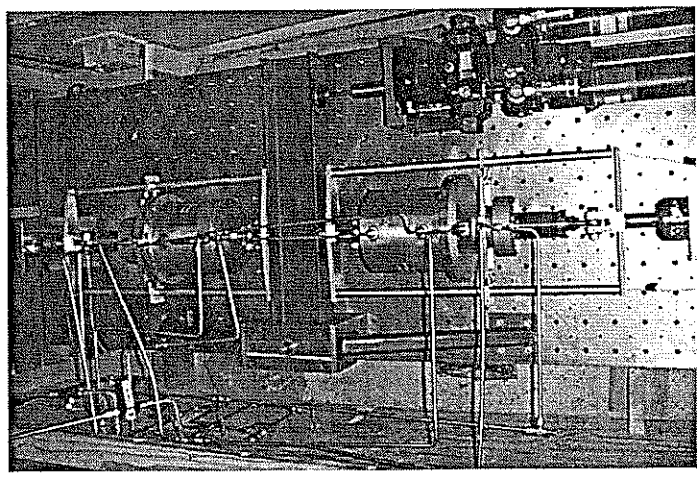

Figure 12. LVIS System testing used cross-linked struts to verify rotational stiffness predictions.

Figure 13 depicts an orbit plot measured under quasi-static conditions, on a strut in the dual-strut cross-linked arrangement. The hydraulic actuator was commanded to provide a mean tensile bias load near 1500 $lb_f$. While the actuator was under displacement control, the strut stroke is seen to vary throughout the measurement. This is attributed to leakage around the hydraulic seals (the LVIS struts are hermetically sealed and that all references to leakage describe fluid flow across seals internal to the strut, and not leakage to the outside environment). A high stiffness of roughly 300,000 $lb_f$/inch was achieved as determined from the slope of the major axis of this orbit.

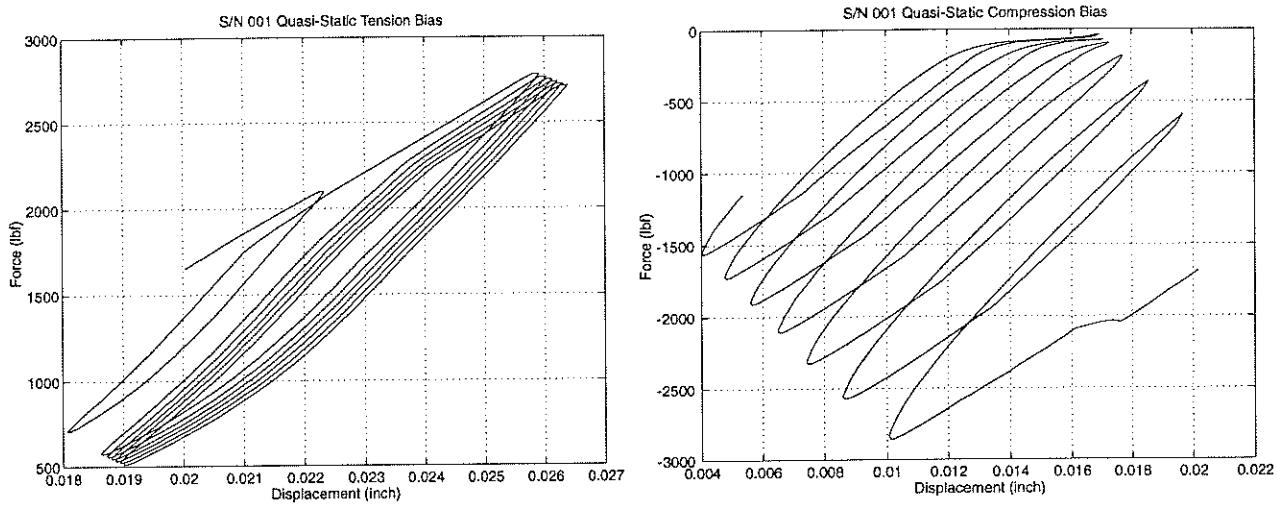


Figure 13a & b. Quasi-Static orbit plot - tensile and compressive biases respectively.

Figure 13b shows an orbit plot measured with the same strut with a compression bias. The apparent effects of seal leakage have a dramatic effect on the strut's performance in this direction. It should be noted that due to the cross-linked nature of the test article, seal leakage in the strut not instrumented will also affect the measurement.

Figure 14 shows an orbit plot measured with a 5 Hz sine input to cross-linked test fixture. The strut stiffness is approximately 330,000 $lb_f$/inch. The area inside the orbit is quite small: the damping in this configuration is low. In the cross-linked configuration, the fluid flow is extremely small due to the "locked-up" condition, unlike that during the pneumatic spring characterization tests. The high system level cross-link stiffness measurements (300K and 330 Klb/in) exceeded our analysis predictions (by a factor of 2), and our greatest expectations; it is not known for sure why the values are so high. Additional work is planned for Phase II to continue developing methodology for predicting the cross-link stiffness more accurately. The results from system level cross-link stiffness testing confirm cross-linking serves its purpose making the 5 Hz axial isolating PAF feasible.

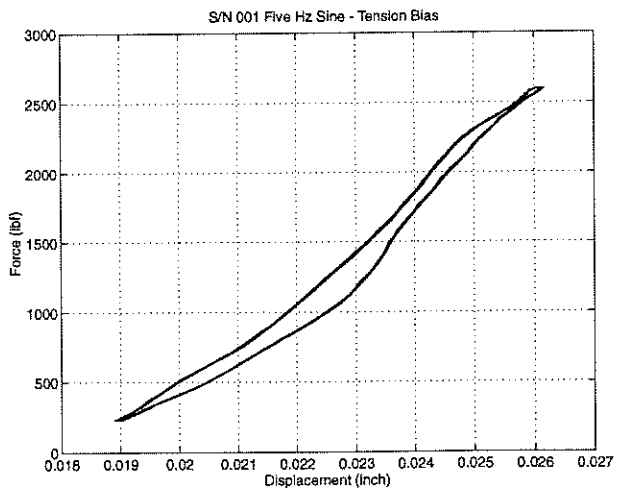


Figure 14. Five Hz orbit plot - tension bias

The hydraulic cross-link damping system performance testing revealed several unexpected results. First, it was noted during the break-in test that a single strut was producing larger than expected damping forces. The damping forces seemed to be increasing with the square of velocity instead of our design goal of a linear velocity relationship ($F_d = CV^2$ vs. $F_d = CV$), indicating turbulent fluid flow.

The unpredicted large damping force was first attributed to the large number of valves and bends that made up hydraulic test set-up. Testing with a smoother loop with less fittings showed some improvement in linearity. After further investigation, we found that the flow was turbulent rather than laminar as predicted. A Reynolds number check verified turbulent flow conditions (peak Re ≈ 40,000 for the test strut, but a value of Re < 2300 is required for laminar flow). Design changes to reduce the Reynolds number include increased tubing and line diameters to slow fluid flow velocities, and increased fluid viscosity.

The struts also exhibited an unusual force vs. displacement behavior during testing with small strokes (~0.05 in) and at higher frequencies. The strut showed a reduced force with displacement followed by a steep load change when the fluid flow is reversed, followed by lower dynamic stiffness once the fluid has been accelerated. This effect was also attributed to the turbulent nature of the dashpot, although no calculations have been made to verify it. A brief explanation on what has been theorized as occurring in the damping system at these higher frequencies follows.

As the hydraulic piston strokes, it forces fluid back and forth through the cross-link line. The force needed to push the fluid through the line is much greater when the flow is turbulent, as the flow in the cross-link lines was for this test. These high flow forces combined with the oscillatory motion of the piston and fluid causes a momentary increase in stiffness during direction changes. The high-stiffness region is then followed by a sloshing surge once the fluid is accelerated, showing up as a low and in some cases negative stiffness region on the orbit plot. We believe that this effect will be minimized by making the cross-link line flow laminar as outlined earlier.

**Summary of Results of Testing.** Table 1 lists the results of the LVIS component and system-level testing carried out. The Phase I test struts were designed to help validate the important ideas of a high-capacity air spring isolator combined with a rotational-stiffening hydraulic cross-link damping system. To save time and cost, the Phase I strut design did not utilize exotic materials or expensive long-lead items. These struts simply allowed us to successfully demonstrate these concepts, the first step towards building a flight-worthy LVIS system. The results indicate that we have been very successful in demonstrating the desired performance.

Table 1. Performance specifications and measured test data for the LVIS Phase I test strut

| Performance Parameter | Design Goal | Measured Value | Comments |
|---|---|---|---|
| Static Stiffness | 3,970 $lb_f$/in | 4,000 $lb_f$/in | 5 Hz axial resonant frequency |
| Cross-Link Stiffness | 400 $klb_f$/in | 300 - 330 $klb_f$/in | Limits payload rocking motion |
| Damping | 107 $lb_f$·s/in | 107 $lb_f$·s/in at low frequency | >20% of critical, $v^2$ damping will be eliminated in Phase II |
| Quasi-Static loading | 7,500 $lb_f$ | 7,500 $lb_f$ | 6.5 g axial loading. Limited to 5500 $lb_f$ due to test facility |
| Max. Cross-Link Load | 4,000 $lb_f$ | 4,000 $lb_f$ | Load per strut caused by max. dynamic moments (twice CSA estimate) |

The basic functionality and structural integrity of the Phase I struts was as designed — extremely durable and robust. The LVIS Phase I test struts have performed as intended and have given us a clear indication that we can proceed with confidence.

## 5. ACTIVE SYSTEM MODELLING

The LVIS effort simulated the effects of an active control system and carried out a trade study to obtain a quantitative evaluation of potential increased payload isolation performance. Our efforts focused on determining how actuator performance requirements (including force magnitude, direction, and the rate of application) affect various spacecraft displacements and accelerations induced by disturbances such as liftoff, transonic and upper atmosphere winds, main engine cut off, etc. Variable control forces were applied at the same locations and parallel to the struts shown in Figure 2, in response to disturbances.

Figure 15 shows the Multiple-Input Multiple-Output (MIMO) control system design topology evaluated. There were 13 inputs: five disturbance inputs $u_d$ and eight active control inputs $u_c$ from actuators located within the PAF. Three outputs $y$ were used for the preliminary evaluation which included the $X$, $Y$, and $Z$ spacecraft bus positions (on top).

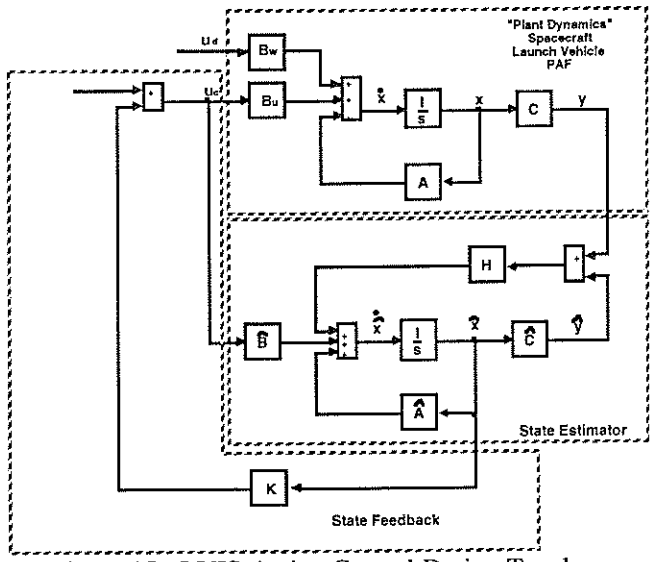


Figure 15. LVIS Active Control Design Topology

The state estimator shown in Figure 15 was used to estimate the states associated with the most important structural modes from a limited number of measurement outputs $y$. The estimator is required because the direct measurement of all modes of interest isn't cost-effective or operationally efficient. We found that 44 states (22 modes) between 1 and 40 Hz were significant based on frequency response comparisons between the plant model and the reduced-order state estimator. The state estimator is defined by the $\hat{A}$, $\hat{B}$, and $\hat{C}$ matrices shown in Figure 15.

Efforts focused on evaluating different methods of calculating the state feedback gain matrix$K$ and the quantitative trade with actuator requirements and isolation performance. These methods include eigenstructure assignment/pole placement and Linear Quadratic Regulator (LQR)/optimal control approaches. This provided the information necessary for trade studies considering force magnitude and bandwidth vs. control system cost and mass.

## 6. CONCLUSIONS

The LVIS program has carried out analytical simulations and testing which indicate significant benefits to the payload, including reduced vibration levels. For a passive 5 Hz axial system, RMS vibration levels were reduced to 20% and 40% of their previous levels over the frequency ranges of 20–40 Hz and 0–40 Hz respectively.

Testing showed that components could be made to provide a 5 Hz axial system while at the same time having very high rocking stiffness. Measured stiffnesses were close to the program goals, and several lessons were learned to improve the design of the struts.

In the active control case, factors of 30 to 100 times improvement were achieved for all isolation performance metrics evaluated for the lift off case. For the Pre-MECO case, factors of 5 to 120 times improvement were achieved.

A quantitative cost evaluation in terms of mass and power of the active control system was made. The degree of isolation performance is related to controller complexity, type of feedback signals used (acceleration, velocity, position, integrated position error), and levels of gain used for each feedback signal. These parameters in turn determine the necessary force, power, and bandwidth requirements of the actuation system. Finally, actuation force, power, and bandwidth determines the mass and cost of a specific actuation system implementation.

An integrated cold gas hydraulic blowdown system can achieve the above mentioned performance improvements (factor of 5 to 120) for approximately 30 to 35 $lb_m$ (actuation and computing) and 15-30 watts of power (sensing and

computing). The consideration of an active control system is merited due to the extremely large performance gain for a relatively modest increase in mass.

## 7. ACKNOWLEDGEMENTS

This work was supported by the U.S. Air Force Phillips Laboratory under contract F29601-95-C-0192.

---

## 8. REFERENCES

1. D. Edberg, C. Johnson, L. Davisc, E. Fosness, "On the Development of a Launch Vibration Isolation System," (with P. Wilke, T. Davis), *Proceedings of the SPIE Smart Structures Conference*, 3-6 March 1997, San Diego, CA.

2. Boeing, *Delta II Payload Planner's Guide*, `http://www.boeing.com/defense-space/space/delta2/guide/delta2.pdf`.